

A Fuzzy-Based Reconstruction Algorithm for Estimating Metal Fill Profile in Lost Foam Casting

W. A. Deabes, *Student Member, IEEE*, M. A. Abdelrahman, *Senior Member, IEEE and ISA*
and P. K. Rajan, *Fellow, IEEE*

Abstract—Lost foam casting (LFC) process is one of the most energy efficient casting methods in the industry. The metal-fill profile is an important factor that affects casting quality. Hence the characterization and the control of the metal fill, if possible, are essential in LFC. Electrical capacitive tomography (ECT) sensors, based on measuring the change in the coupling capacitance with the presence of grounded metal in its proximity, provide a simple non-intrusive visualization technique of acquiring the metal profile. The principle of ECT is to use a rugged and noninvasive array of capacitive electrodes mounted around a target area and measure the changes in inter-electrode capacitance caused by variations of the grounded metal inside the target area. Cross-sectional images of the metal distribution are then reconstructed from the measured data. Deducing the metal fill distribution from the capacitance measurements is a difficult problem. A novel technique for solving the inverse problem in the electrical capacitance tomography is introduced. The new technique is based on Fuzzy Inference Systems (FIS) to predict the molten metal profile from the capacitance measurements. The developed system is intended to be utilized on the foundry floor and hence a limited number of measurements are utilized. The proposed technique is able to detect the position of the metal by using just eight measurements from the sensors.

I. INTRODUCTION

THE Lost foam casting (LFC) is a casting process that uses foam patterns as molds. It is very simple and inexpensive to cast very complex patterns using this process. In the lost foam casting process the molten metal decomposes the foam pattern and creates a casting in its shape [1]. Compared to conventional sand casting processes, this casting method offers significant energy and environmental advantages such as simplified production techniques and reduced environmental waste due to binder system emissions and sand disposal, beside the cost advantages. The process is well known for casting complex geometries, small details, and smooth surface finishing requirements. Another

advantage of using the LFC is that the machining times are significantly reduced if not completely eliminated.

A better understanding of the characteristics of the molten metal inside the foam pattern is needed to reduce the fill related defects and to improve the quality of the final casting [2]. Much effort has been put into developing a wide variety of imaging techniques for industrial process applications over the past two decades. For example, X-ray techniques [1] are presently used to assess the filling characteristics of the liquid metal [3], [4]. However, X-ray methods suffer from the natural hazards of radiation and big size of the equipment. Electrical capacitive tomography (ECT) techniques are gaining increased acceptance for a number of process applications, especially online monitoring and control, due to their noninvasive nature, high data acquisition speed, low construction cost, and safety of operation [5], [6]. ECT system is usually built by installing a number of individual capacitive electrodes around a domain of interest and measuring the change of the coupling capacitance between each pair of these electrodes. In our application, this capacitance measurement is a function of the amount of the grounded molten metal inside a domain of interest [7].

There are two major computational problems in ECT: the forward problem and the inverse problem. The forward problem is to determine inter-electrode capacitances from the permittivity distribution by solving the partial differential equations governing the sensing domain. The inverse problem is to determine the permittivity distribution from capacitance measurements. The result is usually presented as a visual image of the permittivity distribution, and hence this process is called image reconstruction [9]. A tomographic image is reconstructed from the measured signals using image reconstruction algorithms [8]. The linear back-projection (LBP) algorithm is the most popular algorithm for image reconstruction. However, the image obtained by the LBP is blurred with a smoothing effect when a sharp transition between the different dielectric constants is encountered.

In this work, we introduce a novel approach for reconstructing the profile images of the liquid metal inside the foam patterns in the lost foam casting process based on a fuzzy inference system (FIS). The algorithm is divided into three stages as shown in Fig. 1. The 1st stage is pre-processing stage to filter and normalize the capacitance measurements in such a way that they can be applied as inputs to the fuzzy system. The 2nd stage is the fuzzy

This work was supported in part by the Department of Energy, Office of Industrial Technologies under Grant #DE-FC36-04GO14228 and by the Center for Manufacturing Research, Tennessee Tech. University.

W. A. Deabes is currently a PhD student in the Electrical and Computer Engineering Department, Tennessee Tech University, Cookeville, TN 38505 USA (e-mail: wadeabes21@tntech.edu).

M. A. Abdelrahman is with the Electrical and Computer Engineering Department, Tennessee Technological University, Cookeville, TN 38505 USA (e-mail: mabdelrahman@tntech.edu).

P. K. Rajan is with the Electrical and Computer Engineering Department, Tennessee Technological University, Cookeville, TN 38505 USA (e-mail: pkrajan@tntech.edu).

inference system, which takes n capacitance measurements and generates $m \times m$ outputs representing the amount of metal in each pixel in an image, where n is the number of the capacitive measurements, $m \times m$ is the resolution of the final image. The post-processing stage is the last stage to detect the metal position and compute the amount of the metal. The metal location and amount of the metal are used to produce a 2D image describing the metal profile inside the foam pattern.

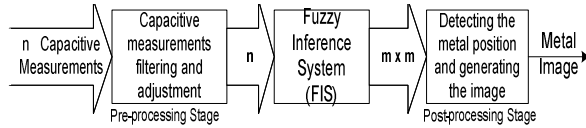


Fig. 1. Block diagram of the fuzzy system for detecting the metal profile.

The paper is organized as follows. Section II is a brief overview of the electrical capacitance tomography technique with investigation of the differences in the hardware implementation and the mathematical model between the regular ECT system and the system proposed in this paper particularly for monitoring the liquid metal. The structure of the sensor array is stated, followed by the calculation of the sensitivity matrix. The new FIS technique for estimating metal profile is described in Section III. Preliminary results and analysis are discussed in Section IV, and conclusions are drawn in Section V.

II. ECT MODEL

A. Sensors Structure

The use of capacitance sensors for detecting the metal profile is different from the general model of the ECT systems especially in the measuring process. ECT system generally consists of an array of electrodes mounted on the periphery of the process vessel needed to be imaged. The electrodes are externally shielded to eliminate stray capacitance effects [10]. To maintain parallel electric field lines by eliminating their axial spreading, driven guard electrodes are installed between the electrodes which improve the axial resolution and sensitivity of the sensors. The mutual capacitances between the electrodes are measured by exciting one electrode at any time and the remaining electrodes function as detectors. The mutual capacitance between the source electrode and the remaining detector electrodes are measured for all the possible pairs. Subsequently, the next electrode is made as source and the same measurement process is employed [11], [12]. For an ECT system having n electrodes, the number of independent inter-electrode capacitance measurements is $n(n-1)/2$. For example, the number of the independent measurements is 120 for 16 electrodes. This measuring protocol is complicated in the hardware implementation due to the multiplexer which used to multiplex the ground and the source signal on each probe. The difference between the modified ECT system used to capture the metal profile and the regular ECT system is mainly in the simplicity of the

measuring protocol. Fig. 2 shows the cross-sectional view of the ECT measurement system which was used to detect the metal profile in the lost foam casting process [2]. An array of 16 electrodes (8 capacitance sensors $S1$ to $S8$) is mounted uniformly around three edges of the foam pattern which will be replaced by the molten metal. A physical limitation prohibits the distribution of sensors around the fourth edge of the foam pattern. This side is used to empty the container from the sand and the final casting after pouring which prevents installing sensors in this part of the container. The imaging area is the boundary of the foam pattern because the metal lies inside this border. Each pair of electrodes works as one capacitance sensor ($S1$ to $S8$), one electrode acts as a transmitter connected to the source signal and the other electrode works as a receiver. Simultaneously, all the transmitters in the eight sets are connected to the source voltage signal with different frequencies and the 8 measurements are captured from all the sensor sets. This makes the setup extremely portable and flexible. A wireless version of the system based on Mote-technology has been developed at TTU which further simplifies the system utilization.

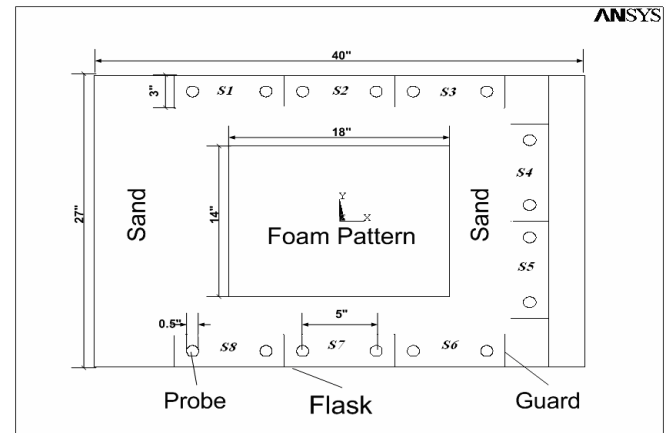


Fig. 2. Planer cross-sectional view of the ECT measurement system with eight sensors.

Figure 2 shows the foam pattern embedded in compressed sand inside a metal container called flask. The outer screen (flask) is connected to the earth to prevent disturbance from outside environment. The grounded radial screens (guards) between the sensor sets ($S1 \dots S8$) reduce the high inherent capacitance between the adjacent electrode probes to enlarge the dynamic range of the sensors and to keep the electrical field as uniform as possible. In Fig. 3, the electrical field

TABLE I
MODEL DESIGN PARAMETERS

Parameter	Value
Relative permittivity of sand	$\epsilon_s = 4$
Relative permittivity of foam	$\epsilon_f = 1.05$
Thickness of electrodes	$R = 0.5''$
Length of guards	$GL = 4.5''$
Electrode separation distance	$D = 3''$

distribution of the given finite element analysis model is shown. A constant voltage (10V) is applied on the transmitters while at the same time the flask, the guards and all the receivers are connected to the ground. All the model design parameters are listed in Table I.

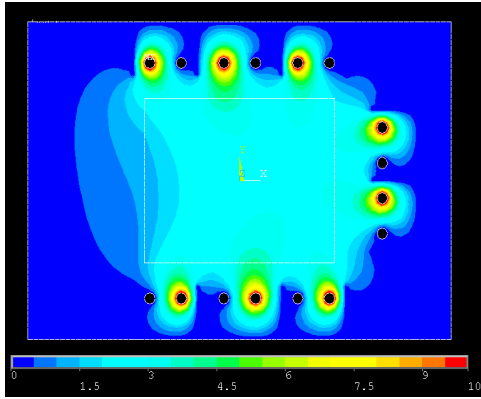


Fig. 3. Electrical field distribution for capacitance sensors.

The geometrical parameters such as the distance between the electrodes, the distance between the foam pattern and the electrodes, and the thickness of the probes have a large effect on the response of the sensors. In order to have a reasonable design to get uniform sensitivity, the geometrical parameters should be selected carefully.

B. Mathematical Model of the Forward Problem

The forward problem is the process of determining the response of ECT sensors given the grounded metal distribution in the region of interest. In regular ECT systems, the relationship between capacitance and permittivity distribution can be characterized by Poisson's equation [7]:

$$\nabla \cdot (\varepsilon(x,y) \nabla \varphi(x,y)) = -\rho(x,y) \quad (1)$$

and the associated boundary conditions (the Dirichlet boundary conditions) imposed by this measurement technique, when electrode i is the source electrode ($i=1,2,\dots$), are

$$\psi^i = \begin{cases} V_c & (x,y) \subseteq \text{all } \Gamma_i \\ 0 & (x,y) \subseteq \text{all } \Gamma_k (k \neq i) \text{ and } (x,y) \subseteq (\Gamma_s + \Gamma_{pg}) \end{cases} \quad (2)$$

where $\varepsilon(x,y)$ is the permittivity distribution in the sensing field, $\varphi(x,y)$ is the electrical potential distribution, and $\rho(x,y)$ is charge distribution. The free charges in the imaging domain are zero which means $\rho(x,y)=0$ and Poisson's equation is converted to Laplace's equation applied on the same boundary conditions. $\Gamma_1, \Gamma_2, \dots, \Gamma_n$ represent the spatial locations of the n electrodes, Γ_s is the

sensor screen, and Γ_{pg} is the n projected guards. So, the boundary conditions are kept constant and when the permittivity distribution changes the mutual capacitance will change. This is, however, different in case of metal fill imaging. By grounding the molten metal, the changing in the solution of Laplace's equation are the boundary conditions that depend on the amount of grounded metal around the sensor inside the imaging area. The boundary conditions in (2) will be changed to

$$\psi^i = \begin{cases} V_c & (x,y) \subseteq \text{all } \Gamma_i \\ 0 & (x,y) \subseteq \text{all } \Gamma_k (k \neq i) \text{ and } (x,y) \subseteq (\Gamma_s + \Gamma_{pg} + \Gamma_e) \end{cases} \quad (3)$$

where, Γ_e represents the spatial locations of the m elements where grounded metal has replaced the foam in the finite element model. Thus, the difference between the regular ECT system and the proposed system to detect the metal profile, from electrical point of view, is changing the boundary conditions depending on the location of the grounded metal and the permittivity distribution in the region of interest.

Equation (4) is known as the forward problem equation of ECT in which the capacitance is calculated for a given permittivity distribution and boundary conditions.

$$C_{ij} = \frac{1}{\Delta V_{ij}} \iint_{\Gamma_j} \varepsilon(x,y) \nabla \varphi(x,y) d\Gamma_j \quad (4)$$

where ΔV_{ij} is the voltage difference between the source electrode and the receiving electrode. Analytical approaches are suitable for solving forward problems for ideal geometries with simplified assumptions; numerical approaches such as finite-element methods (FEM) are used to calculate the sensitivity matrix which represents the response of the sensors by changing individually each element inside the foam pattern from foam to grounded metal.

The main idea of the Finite Element Method (FEM) is that the problem field is divided into a series of elements which are connected to each other only by nodes, and unresolved quantity of internal points in the elements can be obtained by interpolating based on the selected function relationship. The FE model is exploited to obtain the electrical capacitance measurements between electrode pairs by changing each element from foam to metal.

The linearized and discrete form of the forward problem can now be expressed as

$$\Delta C_{m \times l} = S_{m \times n} \Delta H_{n \times l} \quad (5)$$

where, S is a sensitivity matrix, ΔC is the capacitance measurements vector, ΔH is a vector representing the change in boundary condition due to change in the metal fill,

m is the number of the measurements, and n is the number of elements inside the imaging area which is equal to 256 in the model used in this paper. By this approximation, the non-linear forward problem has been simplified to a linear problem [7], [8].

Fig. 4 shows the finite element model of the metal fill problem by using ANSYS software. It shows the domain of solution divided into a number of elements. In order to visualize the metal distribution, the sensing area is divided into N elements or pixels, typically of the order of 2000. In our model the foam pattern, the imaging area, is divided into 16×16 grid generating 256 pixels, and the total number of elements in the whole model is 2370.

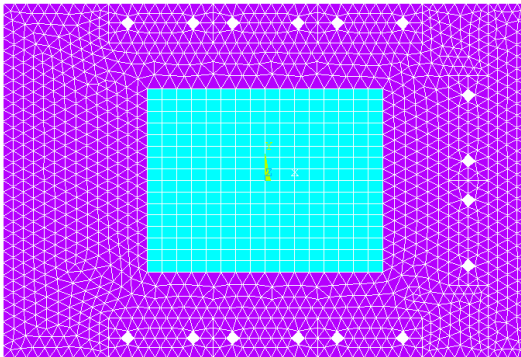


Fig.4. Finite element model of the metal fill problem.

C. Sensitivity Matrix

In the proposed fuzzy reconstruction technique, a sensitivity matrix is used in the generation of the fuzzy rule base as described in the next section. The effect of each element on a certain sensor should be calculated by keeping all the elements as foam and then replacing one element k by metal. This could be done by connecting the element k to the earth and keeping the rest of the elements as floating; then the FEM is used to compute the corresponding electrical capacitance values $C_j(k)$ ($j=1,..,n$).

Finally, eight typical distributions of sensitivity matrix are respectively calculated according to (6)

$$S_i(k) = \frac{C_i^F - C_i^k}{C_i^F - C_i^M} \quad (k=1,2,\dots,n; i=1,2,\dots) \quad (6)$$

where, n is the number of elements inside the foam pattern, C_i^F is the capacitance measurement when the imaging area is completely covered by the foam pattern, C_i^M is the capacitance when the metal completely fills the foam pattern, and C_i^k is the capacitance value after replacing element k in the foam pattern by grounded metal.

Fig. 5 shows the sensitivity matrix for sensors 1 to 4. According to Fig. 5, the response is very high near the sensor and decreases gradually by moving further from the sensor set. The rest of the elements around the imaging area have zero sensitivity because these correspond to the sand

elements where there is no metal. The sensor array is symmetric around axis x along the foam pattern (see Fig. 2), so four sensitivity maps are calculated for the upper sensors ($S1-S4$), and the maps for the rest of the sensors ($S5-S8$) can be derived from these by rotational transformations. So, the sensitivity maps for sensors ($S4-S5$) are equal to the sensitivity maps of sensors ($S1-S4$) after rotating 270 clockwise.

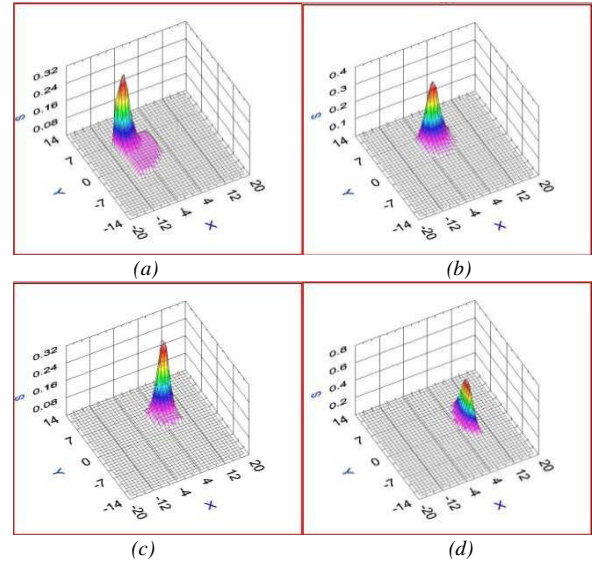


Fig.5. Four sensitivity matrices for a symmetrical eight capacitance sensor array system, all dimensions in X and Y directions are in inches. (a) Sensitivity matrix for sensor 1. (b) Sensitivity matrix for sensor 2. (c) Sensitivity matrix for sensor 3. (d) Sensitivity matrix for sensor 4.

III. FUZZY ALGORITHM FOR THE RECONSTRUCTION OF FILL PATTERN

A novel reconstruction technique using the fuzzy inference system is proposed in this paper. The algorithm consists of three stages.

A. Pre-processing Stage

The measurements vector consisting of 8-measurments $C = [C_1 C_2 \dots C_8]$ should be normalized by using the measurements when the imaging area is all foam and after replacing it all by grounded metal

$$C_N = \frac{C_i^F - C_i}{C_i^F - C_i^M} \quad (7)$$

where, C_i^F, C_i^M are the capacitance vectors when the imaging area is entirely filled by foam and metal respectively, and C_i is the measured capacitance data of a certain grounded metal distribution. The range of capacitance measurements changes depending on the distance between the grounded metal and each sensor. For example, if the metal is located very near to one sensor, the normalized capacitance value from that sensor will be very high, almost one, the measurements from the neighbor sensors will be

medium, and the measurements will be very low from the far away sensors, almost zero.

But, the normalized measurements will be very low from all the sensors if the molten metal is concentrated in the middle of the imaging area. So, the measurements should be scaled to fit within the membership functions of the fuzzy system. The adjusted measurements are obtained using equation 8:

$$C_A = \frac{C_N * M_1}{C_N + M_2} \quad (8)$$

where, C_A is the adjusted input measurements for the fuzzy system, M_1 and M_2 are constants selected according to the range of the input measurements.

B. Fuzzy System Architecture

Fuzzy systems play an important role in various applications and possess the property of being a universal tool to manipulate uncertain information. Fuzzy systems are considered an attractive choice for modeling nonlinear and imprecise data, such as inexact measurements because of their robustness, and ability to withstand noise.

The fuzzy system inputs, ($in1, in2, \dots, in8$), consist of the eight measurements from the capacitance sensors. The input range [0 1] is covered by four triangular membership functions. The fuzzy membership functions for the input, "Z-Zero", "L-Low", "M-Medium", and "H-High", are shown in Fig. 6 (a). The capacitance measurements from nineteen different metal distributions consisting of one piece to four pieces, some of them were placed on the circumference of the imaging area and others in the middle, were used to adjust the range for each membership function of the inputs. Thus, the input membership ranges are non-uniform as shown in Fig. 6 (a).

On the other hand, the 256 pixels values, number of the elements in the imaging area, are labeled as outputs ($out1, out2, \dots, out256$) for the fuzzy system. The output range [0 1] is covered by four membership functions as shown in Fig. 6 (b). The fuzzy membership function "Z-Zero" means there is no metal, "L-Low" membership indicates that the amount of metal is low for this output, "M-Medium" represents medium amount of metal, and "H-High" membership corresponding to the maximum amount of metal.

To automate the process of generation the fuzzy rules, the sensitivity matrix for each sensor is divided into regions according to the effect of the elements on the response of the sensor. Fig. 7 shows different sensitivity regions for sensor 2. For each sensor there are three sensitivity regions, first region contains all the elements which give high change in the response of the sensor, second area consists of all the elements that give medium effect, while metal in the third region will give the lowest change in the response of the sensor. For all the 8 sensors, the indexes of the elements in all the regions are captured and are used to generate the

fuzzy rules.

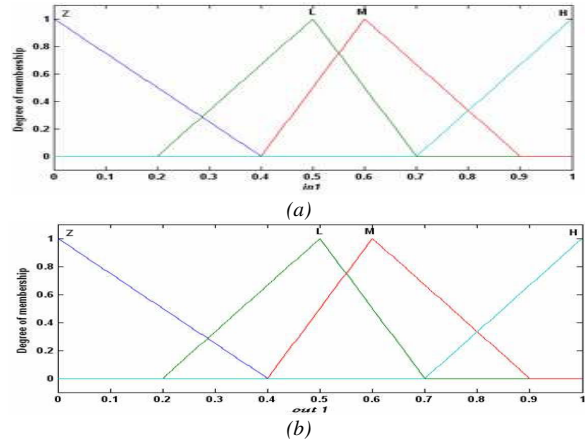


Fig. 6. Membership functions for the fuzzy system inputs and outputs.

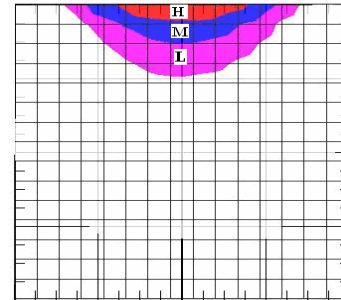


Fig. 7. The different sensitivity regions for sensor 2.

The relationship between one input and the outputs is described by four rules. The fuzzy system has the following simple rule base:

- Rule 1: IF $in_i = Z$ THEN all the elements in the high, medium, and low response regions = Z.
- Rule 2: IF $in_i = L$ THEN all the elements in the high, medium response regions = L.
- Rule 3: IF $in_i = M$ THEN all the elements in the medium response regions = M.
- Rule 4: IF $in_i = H$ THEN all the elements in the high response region = H.

These four fuzzy rules will be repeated for all the inputs, thus the size of the fuzzy rule base is 32.

By taking one case when there is a piece of grounded metal in the corner between sensor 3 ($S3$) and sensor 4 ($S4$), the data from the 8 sensors ($S1, \dots, S8$) can be interpreted by using the fuzzy rules. The data from the eight sensors is shown in Fig. 8 after preprocessing, $S3$ gives the maximum response compared with the other sensors, $S4$ gives medium response because the metal piece is located in its medium effect region, the response from $S2$ is low, and the metal piece is located outside the regions of all other sensors so the response from them is zero. Thus, depending on the generated fuzzy rules, the final outputs are classified as follows: Outputs in the high effect region for $S3$ will be high, the outputs in the medium region for $S4$ will be

medium, the output will be low for the elements in the low region of S_2 , and the rest of the outputs are zero. The 3D final fuzzy result for that particular case is shown in Fig. 9 shows that the high outputs are mainly concentrated in the corner between sensor 3 and 4.

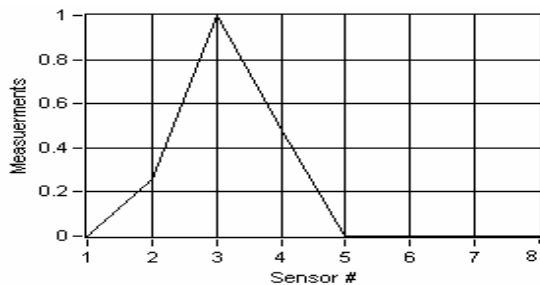


Fig. 8. The pre-processed data from the 8 sensors when a piece of grounded metal exists between sensors 3 and 4.

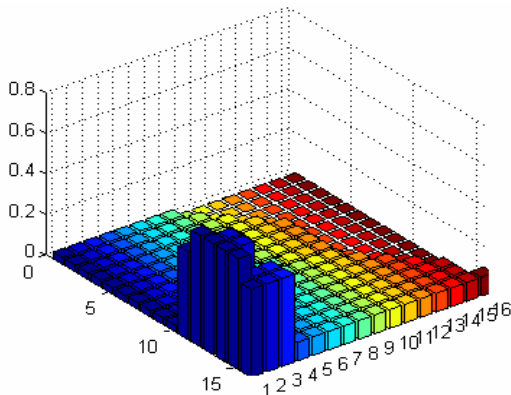


Fig. 9. The 3D final image from fuzzy system when a piece of metal is placed between sensors 3 and 4.

C. Post-processing Stage

In this stage, the 3D image obtained from the fuzzy system in the previous stage is converted into 2D map that shows where the metal is possibly located. A preliminary method for doing this is by dividing the imaging area into 6 regions in front of the sensors in the top and the bottom of the model. A threshold level is applied to the result of the fuzzy system to get rid of all the small values that would affect the computations of the location and the amount of the metal. The centroid for each region is computed to specify the position of the molten metal in this area. In order to compute the amount of the metal, the average is computed for each area. If the average is equal to zero that means the area is empty and there is no metal around that particular sensor. The last step is to plot the amount of the metal at the corresponding centroid.

IV. RESULTS AND DISCUSSION

ANSYS software was used to simulate the lost foam casting model and a LabVIEW toolbox was developed to generate the sensitivity matrix, specify the interest regions for each sensor, implement the fuzzy algorithm

reconstruction technique and plot the final image. Different pieces of metal located in different positions within the sensing domain were used to test the fuzzy reconstruction technique. Fig. 10 shows the actual profiles of the metal in the first column and the final reconstructed results from the fuzzy method in the second column. Fig. 10(a) and 10(b) show the case where there is one piece in front of sensor 1 and 3 respectively. Fig. 10(c) shows the images of the actual metal around sensor 2 and sensor 7 simultaneously. The result shows the ability of the reconstruction technique to detect the location of the two pieces. The most important result is showed in Fig. 10(d) and Fig. 10(e) because the algorithm has detected two pieces of metal located in the center of the sensor array where the effect of the metal is very low from all the sensors, and the sensitivity values are very low. Three pieces of metal were located around sensors S_1 , S_2 , and S_3 at the same time and the result is shown in Fig. 10(f). Fig. 10(g) shows the distribution of four metal pieces located at the corners of the imaging area. The fuzzy technique was able to specify the locations of all the different metal distributions.

In the future work, an improved ECT system will be developed to improve the resolution, and to present the images of the metal fill profile in real time. Another area of improvement would be using iterative reconstruction algorithms for enhancing the results of the current algorithm. It is believed that the ECT system holds significant promise for the future of detecting the profile of the molten metal in the lost foam casting process.

V. CONCLUSION

In this work, a new technique for obtaining the profile of metal using ECT was introduced. The potential application is in the monitoring of metal fill in the casting process. The technique is based on a fuzzy inference system. Simulations were carried out using FEM and used to design and test the FIS. Images for the different metal distributions show that the object position can be discriminated and the inference of the relative object size is possible. The results show that the proposed technique is promising. It is based in a reduced system complexity and reduced number of measurements which is more suitable for its application in foundries.

ACKNOWLEDGMENT

This work was supported by the Department of Energy, Office of Industrial Technologies contract #DE-FC36-04GO14228 and by the Center for Manufacturing Research, Tennessee Tech. University.

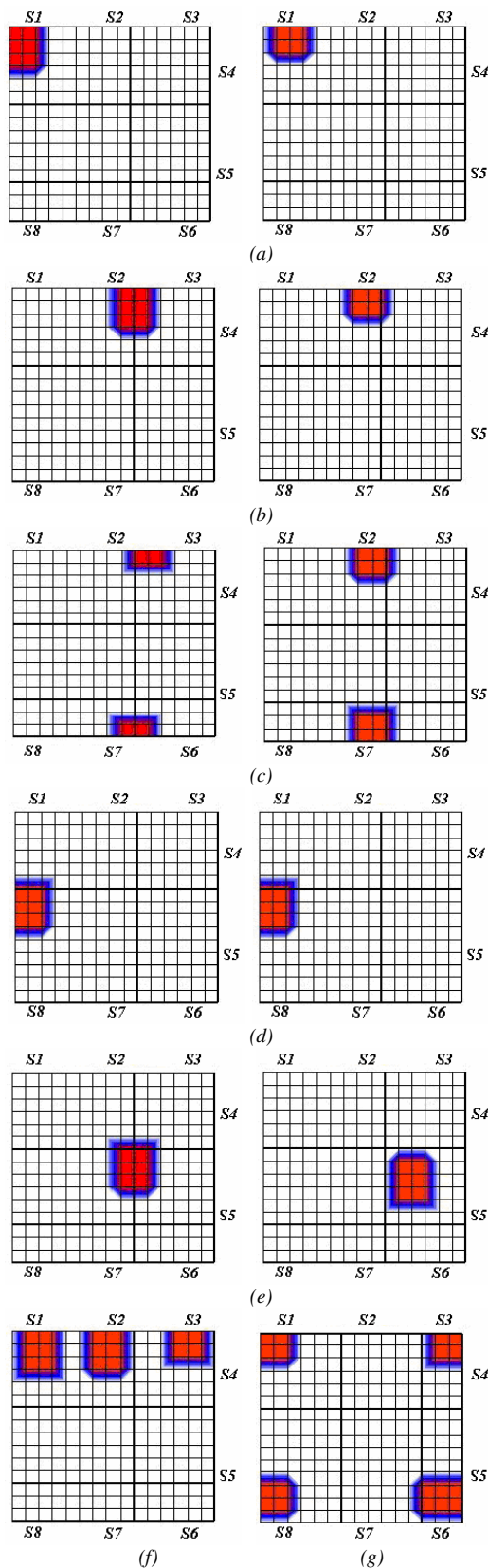


Fig. 10. Reconstruction results using fuzzy technique for different pieces of metal distributions.

REFERENCES

- [1] C. E. Bates, H. E. Littleton, D. Askeland, J. Griffin, B.A. Miller, and D.S. Sheldon, "Advanced Lost Foam Casting Technology", *Summary Report to DOE, AFS*, Report no.UAB-MTG-EPC95SUM, 1995.
- [2] M. Abdelrahmana, J.P. Arulananthama, R. Dinwiddie, G.Walfordc and F. Vondraa, "Monitoring metal-fill in a lost foam casting process", *ISA Trans*, Vol. 45 (4), pp. 459-475, 2006.
- [3] M. Hytros, I. Jureidini, D. Kim, J. H. Chun, R. Lanza, and N. Saka, "A computed tomography sensor for solidification monitoring in metal casting," in *Proc. TMS Annu. Meeting Materials Processing*, pp. 173-181, 1997.
- [4] M. Hytros, I. Jureidini, J. H. Chun, R. Lanza, and N. Saka, "High-energy x-ray computed tomography of the progression of the solidification front in pure aluminum," *Metallurg. Mater. Trans. A*, vol. 30, pp. 1403-1410, 1999.
- [5] C. De-yun, and Z. Gui-bin, "Simulation of sensors and image reconstruction algorithm based on genetic algorithms for electrical capacitance tomography system", *System Simulation J.*, vol.16 no.1, pp. 152-154, January 2004.
- [6] C. De-yun, and Y. Xiao-yan, "The optimized design and simulation of electrical capacitance sensor for electrical capacitance tomography system", *Electronic Measurement and Instrument J.*, vol. 20, no. 1, pp. 22-27, 2006.
- [7] Xie, C.G.; Huang, S.M.; Hoyle, B.S.; Thorn, R.; Lenn, C.; Snowden, D.; Beck, M, "Electrical capacitance tomography for flow imaging: system model for development of image reconstruction algorithms and design of primary sensors", *IEEE Proc-G*, Vol. 139, No. 1, pp. 89-97, Feb. 1992.
- [8] O. Isakson, "A review of reconstruction techniques for capacitance tomography," *Meas. Sci. Technol.*, vol. 7, pp. 325-337, 1996.
- [9] W. Q. Yang and L. Peng, "Image reconstruction algorithms for electrical capacitance tomography," *Meas. Sci. Technol.*, vol. 12, pp. R1-R13, 2003.
- [10] W. Q. Yang, "Hardware design of electrical capacitance tomography systems", *Meas. Sci. Technol.*, vol. 7, pp. 225-232, 1996.
- [11] S. S. Donthi, "Capacitance based Tomography for Industrial Applications", M. Tech. credit seminar report, Electronic Systems Group, EE Dept. IIT Bombay, 2004.
- [12] J. Gamio, "A comparative analysis of single- and multiple-electrode excitation methods in electrical capacitance tomography", *Meas. Sci. Technol.*, vol. 13, pp. 1799- 1809, 2002.
- [13] W. R. B. Lionheart, "Reconstruction algorithms for permittivity and conductivity imaging," in *Proc. 2nd World Congr. Industrial Process Tomography*, Hanover, Germany, pp. 4-11, 2001.
- [14] C.G.Xie, S.M.Huang, C.P.Lenn, A.L.Stott and M. S.Beck "Experimental evaluation of capacitance tomography flow imaging systems using physical models", *IEE Proc. G*, 142(5), pp. 357-368, 1994.
- [15] D. Patil, M. Abdelrahman, W.A. Deabes, and P.K. Rajan, "Characterization of Capacitive Sensors and Monitoring of Metal Fill in Lost Foam Casting", *Thirty-Ninth Southeastern Symposium on System Theory*, pp. 230-235, 2007.